The Journal of Physiology

Standard intensities of transcranial alternating current stimulation over the motor cortex do not entrain corticospinal inputs to motor neurons

Jaime Ibáñez[1,2,3], Blanka Zicher[2], Katlyn E. Brown[4], Lorenzo Rocchi[3,5], Andrea Casolo[6], Alessandro Del Vecchio[7], Danny Spampinato[8], Carole-Anne Vollette[9], John C. Rothwell[2], Stuart N. Baker[10] and Dario Farina[2]

[1] *BSICoS group, I3A Institute, University of Zaragoza, IIS Aragón, Zaragoza, Spain*
[2] *Department of Bioengineering, Imperial College, London, UK*
[3] *Department for Clinical and movement neurosciences, Institute of Neurology, University College London, UK*
[4] *Department of Kinesiology, University of Waterloo, Waterloo, Ontario, Canada*
[5] *Department of Medical Sciences and Public Health, University of Cagliari, Cagliari, Italy*
[6] *Department of Biomedical Sciences, University of Padova, Padua, Italy*
[7] *Department of Artificial Intelligence in Biomedical Engineering, Faculty of Engineering, 17 Friedrich-Alexander University, Erlangen, Germany*
[8] *Non-Invasive Brain Stimulation Unit, Department of Behavioral and Clinical Neurology, Santa Lucia Foundation, Rome, Italy*
[9] *University of Bordeaux, Bordeaux, France*
[10] *Institute of Neuroscience, Newcastle University, Newcastle upon Tyne, UK*

Handling Editors: Kim Barrett & Katalin Toth

The peer review history is available in the Supporting information section of this article (https://doi.org/10.1113/JP282983#support-information-section).

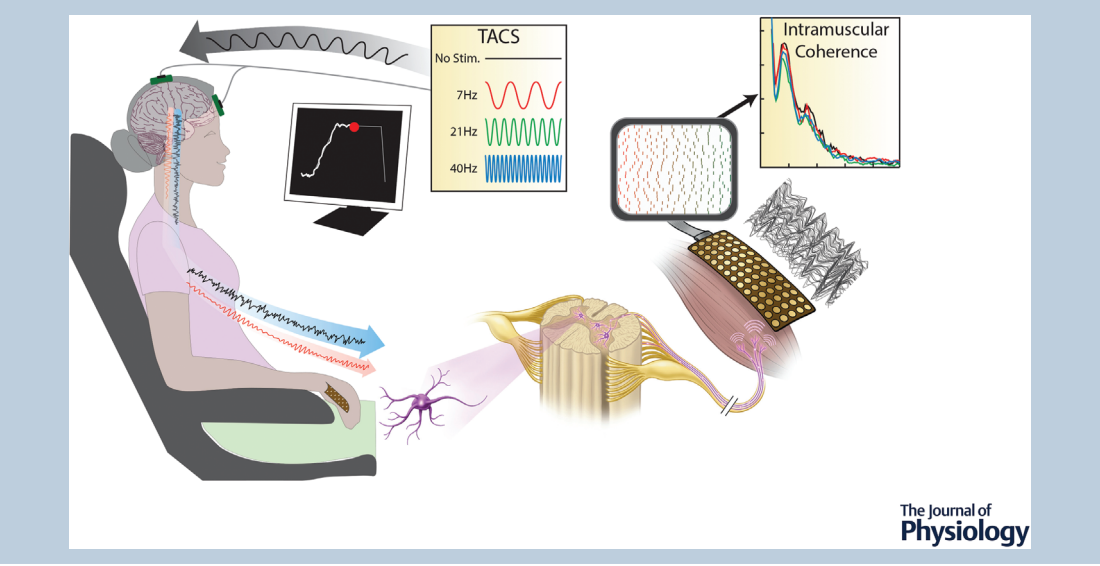

Jaime Ibáñez (Spain, 1984) received a PhD degree in Systems Engineering and Informatics from the University of Zaragoza (Spain) in 2014. He has held postdoctoral positions at the Cajal Institute of the Spanish National Research Council (2014–2016), University College London (UK, 2016–2019, as a Marie-Sklodowska Curie fellow), and Imperial College London (UK, 2019–2021, as senior postdoctoral fellow). He is currently with a La Caixa 'Junior Leader Incoming' fellowship working at IIS Aragón (Spain). His research focuses on biomedical signal processing, movement neurosciences and neurorehabilitation technologies.

J. C. Rothwell, S. N. Baker and D. Farina contributed equally to this work.

DOI: 10.1113/JP282983

Abstract Transcranial alternating current stimulation (TACS) is commonly used to synchronize a cortical area and its outputs to the stimulus waveform, but gathering evidence for this based on brain recordings in humans is challenging. The corticospinal tract transmits beta oscillations (∼21 Hz) from the motor cortex to tonically contracted limb muscles linearly. Therefore, muscle activity may be used to measure the level of beta entrainment in the corticospinal tract due to TACS over the motor cortex. Here, we assessed whether TACS is able to modulate the neural inputs to muscles, which would provide indirect evidence for TACS-driven neural entrainment. In the first part of the study, we ran simulations of motor neuron (MN) pools receiving inputs from corticospinal neurons with different levels of beta entrainment. Results suggest that MNs are highly sensitive to changes in corticospinal beta activity. Then, we ran experiments on healthy human subjects ($N = 10$) in which TACS (at 1 mA) was delivered over the motor cortex at 21 Hz (beta stimulation), or at 7 Hz or 40 Hz (control conditions) while the abductor digiti minimi or the tibialis anterior muscle were tonically contracted. Muscle activity was measured using high-density electromyography, which allowed us to decompose the activity of pools of motor units innervating the muscles. By analysing motor unit pool activity, we observed that none of the TACS conditions could consistently alter the spectral contents of the common neural inputs received by the muscles. These results suggest that 1 mA TACS over the motor cortex given at beta frequencies does not entrain corticospinal activity.

(Received 14 February 2022; accepted after revision 22 June 2022; first published online 1 July 2022)
Corresponding author Jaime Ibáñez: C/Mariano Esquillor Gómez 15, CIRCE Building, 00.260, 50018, Zaragoza, Spain. Email: jibanez@iisaragon.es

Abstract figure legend: TACS over the primary motor cortex may entrain the neural activity in the descending pathways connecting the brain with the spinal cord and muscles. If this is the case, then motor neurons innervating active muscles may reflect such entrainment given their tight connections with corticospinal neurons. We tested this by looking at how the common neural activity in pools of motor neurons projecting to tonically active muscles changed in the presence of TACS at different frequencies. Results from experiments run on humans were combined with simulations using computational models aimed to determine the expected level of sensitivity of motor neuron pools to changes in common inputs. Results indicate that TACS cannot not alter MN activity, which suggests that TACS-driven cortical and corticospinal entrainment may not be easy to achieve at standard intensities used in humans.

Key points

- Transcranial alternating current stimulation (TACS) is commonly used to entrain the communication between brain regions.
- It is challenging to find direct evidence supporting TACS-driven neural entrainment due to the technical difficulties in recording brain activity during stimulation.
- Computational simulations of motor neuron pools receiving common inputs in the beta (∼21 Hz) band indicate that motor neurons are highly sensitive to corticospinal beta entrainment.
- Motor unit activity from human muscles does not support TACS-driven corticospinal entrainment.

Introduction

In humans, transcranial alternating current stimulation (TACS) has been used to entrain the outputs of the stimulated cortical areas and their synchronization with other parts of the nervous system (Helfrich et al., 2014; Paulus et al., 2013; Varela et al., 2001; Violante et al., 2017). However, proof of TACS-driven entrainment is difficult to obtain since direct measurement of brain rhythms non-invasively during TACS is technically challenging (Asamoah et al., 2019; Kasten & Herrmann, 2019; Neuling et al., 2017; Noury & Siegel, 2018; Noury et al., 2016). At present, the extent to which TACS can induce changes in human brain activity affecting the interaction of the stimulated brain regions with other brain or distal networks is unknown.

Animal studies suggest that TACS can acutely entrain cortical neuronal firing, especially when coupled with endogenous rhythmic brain activity (Huang et al., 2021; Johnson et al., 2020). A common form of TACS involves

using stimuli at frequencies matching the beta oscillations (13–30 Hz) that are observed in the motor cortex (Guerra et al., 2016; Nowak et al., 2017; Wischnewski et al., 2019). Importantly, corticospinal cells are involved in the generation of such motor cortical beta rhythms (Jackson et al., 2002). Therefore, if TACS can cause sufficiently strong levels of cortical beta entrainment, this effect is also expected to be apparent in the activity of corticospinal neurons. If this is the case, then, since the corticospinal tract can reliably transmit cortical beta rhythms to motor neurons (MNs) during tonic contractions (Ibáñez et al., 2021), TACS-induced corticospinal beta entrainment may be assessed by studying its distal effects on MNs (Baker et al., 1997; Negro & Farina, 2011a, 2011b). This would provide a novel method to study TACS-driven neural entrainment based on its distal effects, which is especially attractive, as the large separation between cortical stimulation and muscle recordings will minimize contamination by the stimulus artefact.

We tested whether TACS targeting the motor cortex can modulate the inputs received by a pool of MNs innervating a contracted muscle. This would provide indirect evidence that TACS can entrain cortical activity. First, we used a computational model of a MN pool receiving different inputs to assess how reliably the common activity in the MN pool could provide information about changes in corticospinal beta activity (considered a common input to MNs). Then, we ran an experiment in humans aimed to characterize TACS-induced changes in the firing activity of motor unit pools of upper- and lower-limb muscles during tonic contractions. For this, we used high-density electromyography to decompose individual motor unit activity, which inherently eliminates any possible influence of stimulation artefacts on our recordings (because decomposed activity only has information about the times of motor unit spiking, it is immune to contamination from the stimulus artefact). Specifically, to test whether TACS was able to entrain cortical rhythms relayed through the corticospinal tract, we studied whether ongoing levels of common activity in the motor unit pools changed when TACS was delivered. TACS was given at frequencies in the beta band (21 Hz), or at two control stimulation frequencies (7 Hz and 40 Hz) at which no corticomuscular interactions are normally found (Guerra et al., 2016; Williams & Baker, 2009a, 2009b; Witham et al., 2011).

Methods

This study comprises two parts. Part I simulates how the activity of a MN pool changes when the level of beta entrainment of corticospinal common projections to the MNs is modulated. Part II involves experiments using TACS and measuring muscle activity with high-density electromyography (HD-EMG) to measure TACS-driven changes in the neural drive to the muscle by analysing the spiking activity of pools of motor units.

Ethical approval

All procedures and experiments were approved by the ethics committee of University College London (Ethics Application ID 10037/001). The study conformed to the standards set by the *Declaration of Helsinki*, except for registration in a database. Written informed consent was obtained from all subjects prior to the study. None of the participants had contraindications to TACS (Rossini et al., 2015).

Part I – simulation of a pool of MNs receiving common beta inputs

It has been previously shown that cortical oscillations are transmitted to the muscles through the fastest descending pathways (Ibáñez et al., 2021). This implies that, when simulating the activity of MN pools receiving cortical oscillatory inputs, one can use simplified models that only consider the fastest and most direct descending corticospinal projections to MNs. Here we used a computational model of a pool of MNs receiving a common input that simulated the summed contribution of corticospinal neurons, and independent inputs that were different for each MN (Fig. 1). Individual corticospinal inputs were simulated as spike trains with the times of the spikes randomly determined following Poisson distributions. These Poisson distributions had non-constant rate parameter (lambda), determined by summing a constant value (which corresponded to an average firing rate of 25 spikes per second as in previous primate studies (Baker et al., 2001; Williams & Baker, 2009b)) with a sinusoid at 21 Hz (the beta modulation). The amplitude of the sinusoidal modulation was changed to simulate different strengths of beta modulation. The frequency of the beta inputs was set to 21 Hz based on previous studies of corticomuscular beta coherence in humans during sustained mild contractions (Ibáñez et al., 2021). The net common input to MNs was the result of summing the spike trains of 100 corticospinal neurons, which simulated the contribution of the fastest corticospinal projections to the MN pool. The number of corticospinal neurons used was based on the relation between the estimated size of unitary excitatory post-synaptic potentials (EPSP) from corticomotoneuronal projections, and the size of compound EPSPs resulting from stimulating the pyramidal tract (Kraskov et al., 2019; Porter & Lemon, 1995; Williams & Baker, 2009b). The independent inputs to MNs were modelled as white Gaussian noise, with means equal to variance. The level

of the mean was adjusted with reference to preliminary simulations to make MNs fire at an average discharge rate of ∼11 spikes per second, which is a typical average firing rate for motor units active during mild contractions (Ibáñez et al., 2021). The MN model used was a previously validated computational model (Baker & Lemon, 1998; Williams & Baker, 2009a, 2009b). The model is based on a previously published model (Booth et al., 1997). It includes a somatic and dendritic compartment, and eight active conductances found in mammalian motoneurons (soma: gNa, gK(DR), gCa-N, gK(Ca), gNa-P; dendrite: gCa-L, gCa-N, gK(Ca)), each with Hodgkin–Huxley style kinetics. The firing activity of a population of 177 MNs was simulated. The systematic change in excitability with recruitment order was modelled heuristically by changing the fraction of input from the dendritic tree, as described in previous works (Williams & Baker, 2009a). The differential equations governing MN membrane potential were solved using the exponential integration scheme (MacGregor, 1987), with a time step of 0.2 ms. The model was coded and run in MATLAB (version 2020a, The Mathworks Inc., USA).

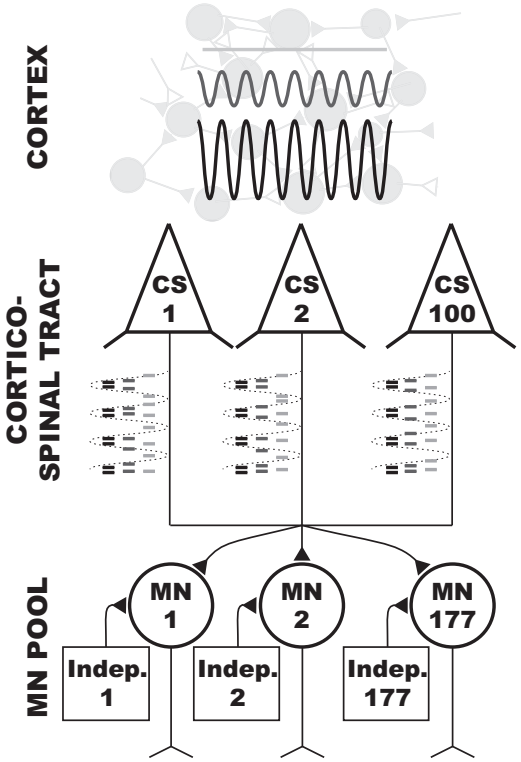

Figure 1. Schematic of the model used in this study
A pool of 177 motor neurons (MNs) receive independent inputs (different inputs to each MN) and a common input simulating the descending neural input from 100 corticospinal neurons (CS) with monosynaptic connection to MNs. The model is used to test how the estimated common inputs to MNs change as a function of the level of entrainment of the corticospinal tract with beta oscillations. Three levels of beta entrainment are exemplified using grayscale.

To study how the activity of MNs changes due to changes in beta entrainment of corticospinal neurons, we ran a series of simulations in which we gradually increased the amplitude of the beta component modulating the discharge rates of the corticospinal neurons. To have a reference value for the amplitude of this beta component (referred to as 'reference beta level' from now on), we considered previous studies on primates looking at the typical values of coherence within the beta band between recordings of local field potentials in layer V of the primary motor cortex and the spike trains of corticospinal neurons (Baker et al., 2003). Based on these works, peak beta coherences should be around 0.02. Therefore, we determined the amplitude of the beta signal (21 Hz) modulating the discharge rate of corticospinal neurons that led to a coherence amplitude of 0.02 between the beta sinusoid and the spiking activity of the corticospinal neurons. The estimated reference beta level was 2.5 spikes per second, that is 10% of the baseline discharge rate of the corticospinal neurons. Based on this level, we ran 100 simulations of 121 s each (with the first second discarded in the analysis), testing increasing levels of beta amplitude from zero (no modulation) to four times the reference beta level. These tests allowed us to model how reliably the spiking activity of MNs can signal changes in beta activity in the corticospinal tract.

We also used the MN model to estimate the expected minimum detectable effect size of experiments in Part II. We ran 100 simulations in which the level of beta modulation of the corticospinal neurons was kept constant at the reference beta level. In this case, the simulated blocks were of 41 s (with the first second discarded) to make them match with the analysed data in Part II. Results were then used to estimate the minimum level of change in the intramuscular coherence (the main outcome measure here, as described below) that should be detectable given the experimental conditions in Part II.

Part II – motor unit activity in contracted muscles during TACS

Here, we analysed how the common activity in pools of motor units innervating upper- and lower-limb muscles changed during TACS. For this purpose, we recruited 10 healthy subjects (nine male; ages 22−40).

Experimental task. Recording sessions comprised two separate blocks in which we collected data from the right tibialis anterior (TA) and abductor digiti minimi (ADM) muscles during isometric contractions and while TACS was delivered over the motor cortex. Figure 2*A* shows the position in which the arm and leg were held during the recordings. At the beginning of each block, the maximum voluntary isometric contraction (MVC) of the studied

muscle was estimated. Each block consisted of four runs in which subjects departed from a relaxed position and followed a path on a screen by producing forces with the measured muscle. The target force path consisted of: (1) a resting period (5 s); (2) a ramp contraction period (5 s) where force was linearly increased to reach a target level of 5% (ADM) or 10% (TA) of the MVC; and (3) 60 s of steady contraction. The different contraction levels required for ADM and TA was based on the different characteristics of motor units in the two muscles, and they were meant to lead to the activation of large enough pools of units without causing fatigue (Enoka, 2008).

Stimulation. The above tasks for the upper- and lower-limb muscles were performed by the subjects while four different stimulation conditions were tested per muscle: no stimulation (No Stim condition) and TACS with an amplitude of 1 mA and at 7 Hz, 21 Hz and 40 Hz (Fig. 2*A*). TACS was delivered through a pair of conductive rubber electrodes adhered to the scalp using conductive paste (model of the stimulator: DC-Stimulator plus, Neuroconn, Germany). One electrode (5 × 5 cm) was placed either over C3 (ADM) or Cz (TA) positions on the scalp based on an EEG cap with a 10/20 layout (Fig. 2*A*). The Pz position was used for the second electrode (5 × 10 cm) to minimize phosphenes (Kar & Krekelberg, 2012). The stimulator was driven by a voltage signal generated by a DAQ board (USB-6229, National Instruments, USA) programmed from a PC. The constant-current stimulator generated electrical currents proportional to the voltage applied by the DAQ. In each run, the stimulation started with subjects at rest, and it continued during the entire duration of the isometric contraction of the muscle sustained for 60 s, from which we analysed the last 40 s. This was done to maximize the number of decoded motor units steadily firing, since some of the identified units started firing some time after reaching the plateau force (Del Vecchio et al., 2020).

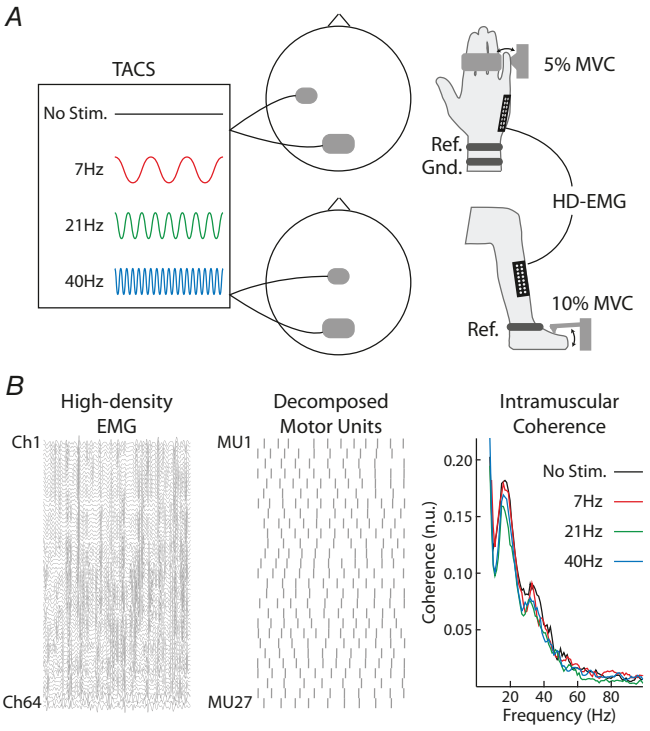

Figure 2. Experimental set up in Part II of the present study and recordings of the common inputs to a muscle using the intramuscular coherence function
A, four TACS conditions were delivered (No Stim. – black; 7 Hz TACS – red; 21 Hz TACS – green; 40 Hz TACS – blue) either over the hand or leg cortical area while isometric steady contractions were produced either with the abductor digiti minimi (ADM) or the tibialis anterior (TA). High-density electromyography (HD-EMG) was recorded from the ADM or TA using 64-channel grids (Ref. – reference; Gnd. – ground position; Gnd. was placed on the wrist also for TA measurements). *B*, HD-EMG recordings were used to extract information about spiking activity of motor units from the contracted muscles. Spiking activity of pools of motor units was used to estimate the common synaptic inputs to the motor neuron pools by computing the intramuscular coherence (see details in *Methods*).

Muscle recordings. HD-EMG grids with 64 contact points (13 × 5 matrices) and an inter-electrode distance of 4 mm (ADM) or 8 mm (TA) were placed centred around the innervation zone of the muscles after skin preparation (preparation involved shaving the skin over the muscle and cleansing with abrasive gel and alcohol wipes with 70% ethanol to minimize electrode–skin impedance; Fig. 2*A*). A bracelet around the distal part of the forearm was used as ground and an additional bracelet around the bony area of the wrist (ADM) or the ankle (TA) was used as the reference. EMG signals were band-pass filtered (20−500 Hz) and sampled at 2048 Hz (Quattrocento, OTBioelettronica, Italy).

Decoding of motor unit activity. HD-EMG signals were decomposed offline into motor unit spike trains using a validated blind source separation procedure (Holobar et al., 2014) (Fig. 2*B*). The estimated motor unit spike trains were then visually inspected and processed following previously proposed guidelines (Del Vecchio et al., 2020; Hug et al., 2021). From the decomposed motor units, only those active throughout the analysed intervals and with a pulse-to-noise ratio of over 30 dB were kept for further analysis (Holobar et al., 2014; Hug et al., 2021). A minimum of six reliably identified units in all runs of a block was set as the criterion to keep recording blocks for subsequent statistical analysis. This was done to ensure that the pools of units considered could reliably characterize common inputs in different frequency bands (Gallego et al., 2015) and it led to discarding the ADM

blocks of three subjects. The resulting pools of motor units were used to characterize the common inputs to muscles.

Analysis of data from Parts I and II: characterization of common inputs from MN activity

To study the common inputs to a MN pool within different frequency bands, we used the intramuscular coherence function (IMC) (Bräcklein et al., 2021, 2022; Farina et al., 2014) (Fig. 2*B*). The IMC was obtained by running 100 iterations of an algorithm that first randomly divided the pool of MNs considered into two sub-pools of equal size, and then calculated the spectral coherence between the cumulative spike trains obtained from the two sub-pools by summing the spiking activity of the MNs in each pool. Coherence was computed using 1 s segments and the multi-taper method for spectral estimation (NW = 2; Neurospec-2.11) (Halliday, 2015; Ibáñez et al., 2021).

In the case of the data obtained from the first simulations in Part I (increasing levels of beta), the IMC was computed using sub-pools of increasing sizes from 1 to 88 MNs and the average IMC levels within the 20−22 Hz band were determined for each level of beta input simulated. From here on, we refer to the number of MNs used per sub-pool for IMC estimation using the expression 'MNs/sub-pool'.

For the data from the second set of simulations in Part I, IMC was computed using seven MNs/sub-pool to approximate the average number of units reliably identified in Part II (on average, ∼13 units were decomposed from the recorded muscles; see results). The mean (μ) and variance (σ^2) of the average IMC in the 20−22 Hz band across the 100 simulations were obtained and used to estimate the minimum detectable effect size (MDES) as follows:

$$MDES\,(\%) = \frac{\sqrt{\frac{\sigma^2\left(z_{1-\beta}+z_{1-\alpha}\right)^2}{n}}}{\mu} \times 100$$

where n is the sample size (17 recordings considered in the main results in Part II), α and ß are the probabilities of type I/II errors, and z refers to the critical Z value (Rosner, 2015). α and ß were set to 0.05 and 0.2.

In Part II, the number of motor units used to estimate the IMC was determined for each subject by considering the block with the lowest number of units decomposed. In this case, we assessed whether IMC amplitudes changed at the frequencies at which TACS was delivered. Therefore, we calculated the average IMC amplitudes within three frequency ranges: 4−13 Hz; 13−30 Hz; 30−50 Hz and used these results to run statistical tests (we also ran analyses using narrow windows of 2 Hz around the stimulus frequencies and they led to results equivalent to those with the broader bands; results not shown). Mixed modelling was used to determine the influence of TACS on IMC. Fixed factors included in the model were TACS stimulus (referred to as STIM; this factor had four possible levels – No Stimulation (No Stim.), and 7, 21 and 40 Hz stimulation), frequency band of analysis (FREQ), and the interaction between the two (STIM × FREQ). Subject was included as a random factor. To test our specific hypotheses regarding the influence of TACS at 21 Hz on beta coherence, we ran pairwise comparisons contrasting the TACS protocols. Results from the two muscles studied were merged for this analysis. We also ran tests using muscle as a factor and muscle-specific tests. These tests led to results (not included in the manuscript) that were equivalent to the main results reported. Assumptions of normality and homoscedasticity of the residuals were assessed visually using q-q plots and fitted- *vs.* residual-value plots. The lmer package (Bates et al., 2015) in R (R Core Team, 2019) was used. All results are reported as the means ± SD (unless specified otherwise) and considered significant if $P \leq 0.05$.

Results

Part I – computational models indicate that MNs can provide reliable information about changes in beta inputs to corticospinal neurons

Figure 3 shows how common inputs to the simulated MN pool are measured by the IMC as the number of MNs considered increases. These results are for the case in which a reference beta level (estimated, as described in *Methods*, based on Baker et al. (2003)) is used to modulate the activity of corticospinal neurons. Although only one sinusoidal component (the beta input at 21 Hz) modulates the common inputs, since corticospinal inputs to MNs are spike trains following Poisson distributions, their spectral contents cover a wide range of frequencies (Dideriksen et al., 2012). Therefore, variable levels of common inputs (i.e. non-zero coherence levels) are observed in the IMC at frequencies outside the bandwidth of the beta input (Fig. 3*A*).

As expected, the amplitudes of the IMC at the frequencies of the beta inputs to the MN pool increase when the size of the sub-pools of MNs used to estimate the IMC increases (Fig. 3*A*) (Farina & Negro, 2015). However, when the IMC is estimated using large sub-pools of MNs, even very small common inputs outside the beta band (that may be spurious and due to chance) can be strongly enhanced by the IMC (as observed in the offset level present in the darkest traces in Fig. 3*A*). This may affect the characterization of actual common inputs (like beta inputs in these simulations), as the range between chance-related IMC levels and the maximum possible coherence of one shrinks. Interestingly, the computation

of the IMC using small-to-medium sub-pools (i.e. 5−15 MNs/sub-pool) results in close to zero coherence levels at frequencies outside the common beta inputs, while coherence at the beta input frequency vary with the input. This is the case, for example, when the IMC is computed using seven MNs/sub-pool (blue trace, Fig. 3*A*), which is the condition that best matches the number of MNs used to estimate the IMC in Part II of this report (∼13 units were decomposed on average across subjects and muscles in the experimental datasets).

Before analysing how the IMC changes with changes in the beta input to corticospinal neurons in our simulations, it is important to assess whether the reference beta amplitude used (based on intracortical recordings in primates; see *Methods*) produces IMC levels in the beta range similar to those observed experimentally. This should be expected if the only, or most dominant, common beta input to the MN pool resulted from a single corticospinal source. This is the case here: the IMC amplitude at 21 Hz increases with the number of MNs used to estimate it, showing an initial steep increase followed by a slower ramp trending towards 1 (Fig. 3*B*). Based on this graph, when the number of MNs used approximates what is typically decoded in human experiments (i.e. estimates of IMC using 10−30 MNs in total, that is, 5−15 MNs/sub-pool) (Del Vecchio et al., 2020), the IMC beta level is approximately 0.1–0.3. This is in line with human recordings during steady contractions (Castronovo et al., 2015; Negro et al., 2016).

The IMC is highly sensitive to changes in the beta modulation of corticospinal neurons. Figure 4 shows how IMC changes with increasing amplitudes of the beta signal modulating corticospinal neurons and when either one, seven or 88 MNs per pool are used to estimate the IMC (Fig. 4*A*–*C*). The amplitude of the IMC at around 21 Hz (frequency of the common beta input) follows the increases in the amplitude of the beta inputs. The number of MNs considered influences how changes in beta inputs are reflected in the IMC. Changes in the IMC when one or 88 MNs/pool are considered are constrained to coherences between 0 and ∼0.4 and ∼0.4 and 1. When the IMC is estimated using seven MNs/pool, the beta IMC resulting

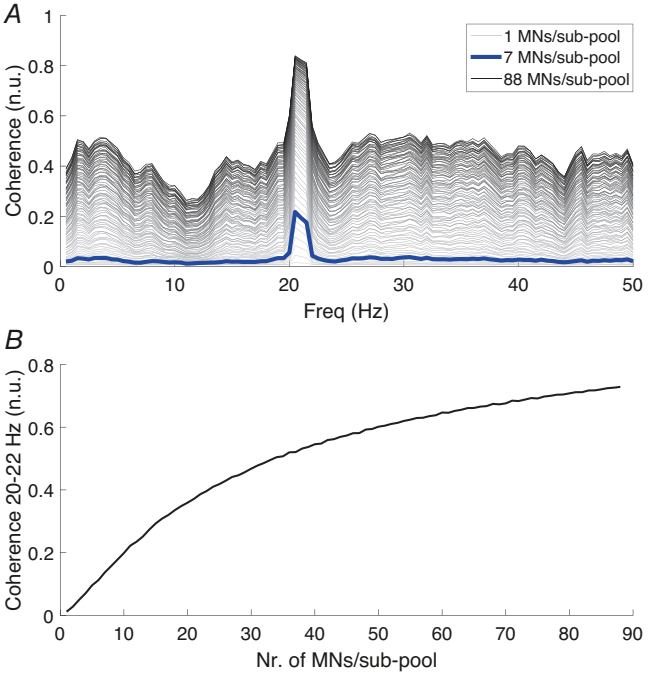

Figure 3. Intramuscular coherence estimated for the case in which a reference beta level is used to modulate corticospinal neuron firing activity
Results obtained using different number of motor neurons per sub-pool (MNs/sub-pool) to estimate intramuscular coherence. *A*, intramuscular coherence in the 0−50 Hz range (from light grey to black, traces represent intramuscular coherence estimates using 1–88 MNs/pool; the case in which seven MNs per pool are considered is highlighted in blue); *B*, average intramuscular coherence in the 20−22 Hz band as a function of the number of MNs used to estimate it.

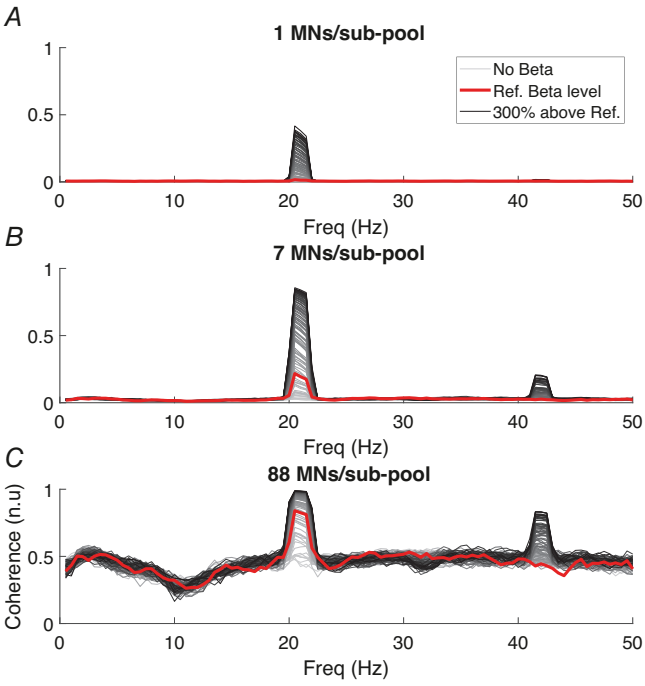

Figure 4. Intramuscular coherence with different amplitudes of the beta signal modulating pyramidal tract neurons projecting onto a simulated pool of motor neurons (MNs)
A–*C*, results for the cases in which one, seven or 88 MNs/pool are considered to estimate the intramuscular coherence. From light grey to black, traces represent the different levels of beta simulated ranging from no beta modulation to a 300% increase in beta relative to the estimated reference beta level. The highlighted red trace represents the intramuscular coherence when the beta signal modulating inputs has the estimated reference beta level.

from different levels of beta inputs range between 0 and ∼0.9.

The IMC changes with the amplitude of the beta signal modulating corticospinal activity. This is shown in Fig. 5 both in absolute terms (Fig. 5*A*) and in terms of changes in IMC relative to levels observed when the reference beta level is used as the input (Fig. 5*B*). These results suggest that small changes in the amplitude of the beta modulation relative to the estimated reference beta level can lead to relatively big changes in the IMC at beta frequencies. As a reference, changes of 8−12% in the amplitude of the beta signal modulating corticospinal activity (relative to the reference levels) should result in changes of approximately 0.015–0.030 in the IMC when 14 MNs (seven MNs/pool) are considered.

Finally, a minimum detectable effect size of 7% was obtained based on the results from the second set of simulations in Part I. This implies that the experimental conditions in Part II are expected to be powered to detect TACS-driven changes in the IMC greater than 7% relative to baseline.

Part II – estimated common inputs to muscles in humans do not change during TACS

Across subjects and muscles, 12.9 ± 4.4 motor units were identified (range 6−22; 9.7 ± 2.4 ADM; 15.2 ± 4.1 TA). The average discharge rate of the motor units during steady contractions was 11.9 ± 2.1 spikes/s. Paired *t* tests run between all tested conditions showed no significant effect of TACS on average forces ($P > 0.3$ in all paired comparisons).

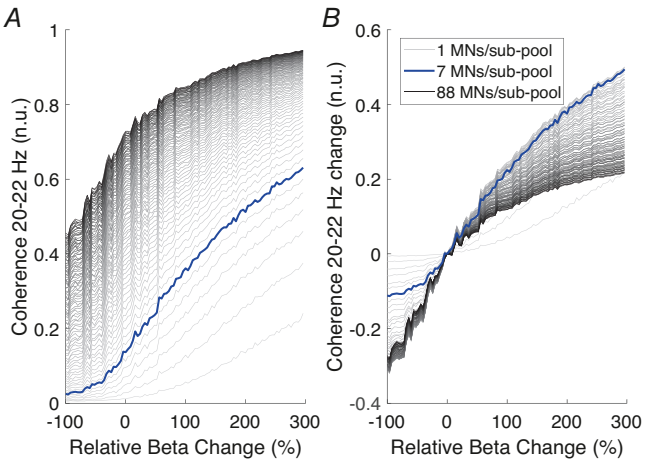

Figure 5. Intramuscular coherence in the 20−22 Hz band as a function of changes in the amplitude of the beta signal modulating the firing activity of corticospinal neurons
A, absolute intramuscular coherence amplitudes as a function of changes in beta inputs. *B*, changes in intramuscular coherence amplitudes relative to coherence when using the reference beta level.

Table 1. Results with the main model used in the study to examine intramuscular coherence changes due to transcranial alternating current stimulation

Model parameter	Sum sq	Mean sq	*F* value	*P* value
STIM	0.016	0.005	0.688	0.560
FREQ	1.754	0.877	118.888	<2e-16*
STIM × FREQ	0.007	0.001	0.149	0.989

There was no significant influence of transcranial alternating current stimulation (TACS) on the intramuscular coherence function, and there was no interaction between the TACS protocol used (STIM) and the frequency band considered (FREQ).

Figure 6 summarizes individual and group IMC results. We did not find differences in the IMC between the tested TACS conditions. Specifically, results from the model examining IMC changes indicated no effect of STIM ($P = 0.56$; Table 1), and no significant STIM × FREQ interaction ($P = 0.99$). Paired comparisons showed a difference between blocks with no TACS and with TACS given at 21 Hz on the IMC levels in the beta band ($P = 0.027$), suggesting that the amplitude of the IMC in the beta band decreased during 21 Hz TACS. However, this significance did not survive *post hoc* correction for multiple comparisons.

As indicated in the *Methods*, analogous tests to the one presented above were also performed considering IMC levels in narrow bands of 2 Hz around the TACS frequencies as well as using muscle as a random factor in the analysis. The main results did not change in any of these cases (results not shown).

Discussion

Finding direct *in vivo* evidence of the effects of TACS on ongoing neural activity in an undamaged human brain is challenging due to technical limitations in existing brain recording technologies (Beliaeva et al., 2021; Noury et al., 2016). Here, we propose a way to infer TACS-driven entrainment by assessing the distal effects that the stimulation has on alpha MNs innervating muscles. The experiments run to test this methodology lead to two contrasting results: while simulations indicate that information from pools of MNs in a muscle can provide reliable information about changes in cortico-spinal entrainment, results from human experiments show that TACS over the motor cortex does not change the spectral properties of the common inputs received by pools of MNs in upper- and lower-limb muscles. Considering the involvement of corticospinal neurons in the generation and propagation of beta rhythms observed in the motor cortex (Jackson et al., 2002), our results also suggest that TACS, with the intensity and montage

used here, does not have a strong effect on motor cortical outputs.

The capacity of TACS to entrain cortical activity in humans has been a subject of debate over recent years. While several animal studies have suggested that cortical activity can be entrained by TACS in a dose-dependent manner (Johnson et al., 2020; Khatoun et al., 2017), other works have argued that the TACS intensities needed to generate intracortical electric fields able to modulate neural activity in humans far exceed what is typically used (and tolerated) (Lafon et al., 2017; Vöröslakos et al., 2018). A key point to interpret these contrasting results is the attenuation of the TACS-induced electric fields when entering the brain and the ability of these weakened fields to condition ongoing cortical activity. Based on our simulations, the assessment of common inputs to MNs in activated muscles should be able to measure relatively small levels of entrainment in the corticospinal tract. However, results from our human experiments suggest that common inputs to motor units remain largely unchanged during TACS. In fact, stimulation with beta frequencies not only did not increase levels of common beta inputs to MNs, but it showed a trend towards the opposite direction (not significant after correcting for multiple comparisons). This lack of evidence for rhythmic entrainment of MNs may be interpreted in different ways. First, our results may indicate that stimulation did not entrain neural activity of, at least, spinal MNs and pyramidal cells connecting to them. This could be due to the use of too low intensities or to a lack of focality and depth in the generated electrical fields with the electrode montage used here. Future studies should be performed to assess whether moderate changes in TACS intensities (keeping stimulation tolerable) and refinements in the electrode montages can lead to observable effects in the entrainment of cortical outputs to MNs (Asamoah et al., 2019; Vöröslakos et al., 2018; Wischnewski et al., 2019). A second explanation may be that entrainment using standard TACS intensities is only possible when the stimulated brain areas are in a dynamic phase (i.e. transitioning between two states), since during these less stable neural states external stimuli appear to be more capable of producing changes in the brain (Fu et al., 2021; Kozyrev et al., 2018). This would explain why we could not find any evidence for corticospinal entrainment here while previous works (relying on measurements of scalp electrical signals during TACS) found significant TACS-driven corticomuscular beta entrainment during

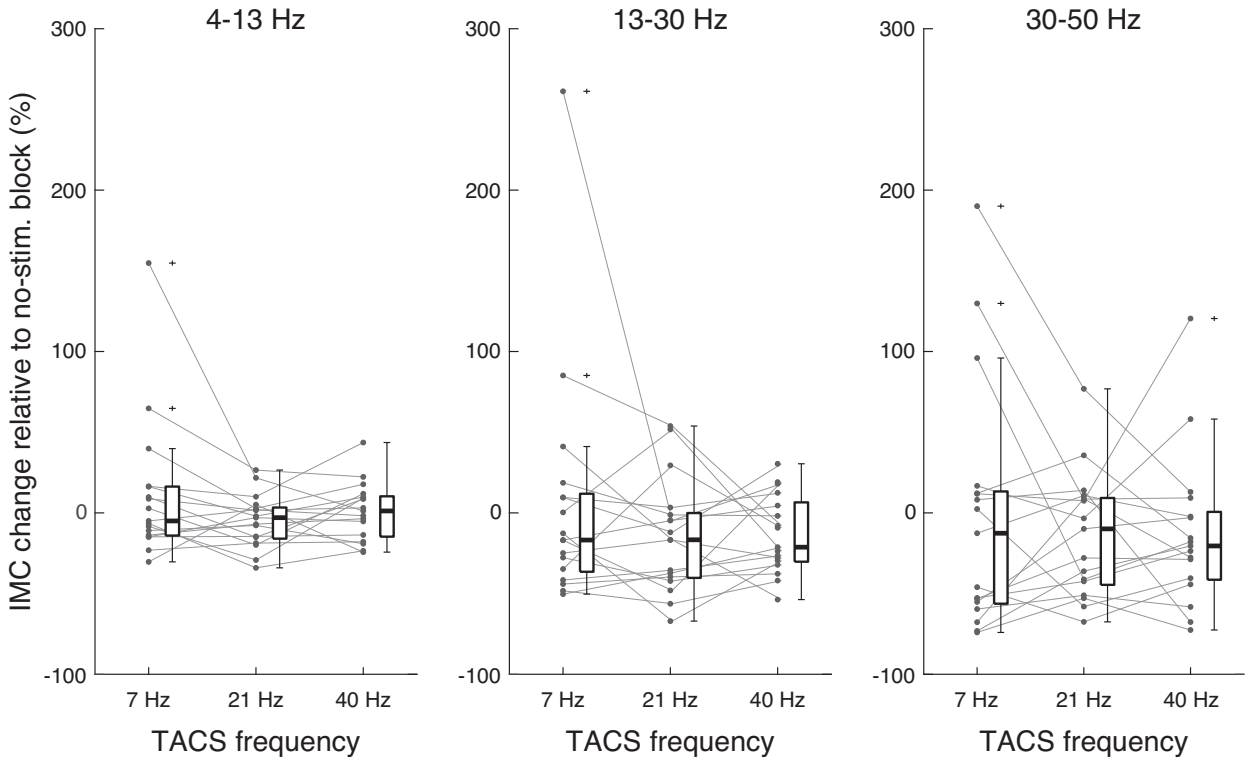

Figure 6. Changes in intramuscular coherence during transcranial alternating current stimulation TACS
Intramuscular coherence changes (relative to No Stim blocks) within three frequency bands of interest and for the three TACS conditions tested: TACS given at 7 Hz, 21 Hz or 40 Hz. Results with tibialis anterior (TA) and abductor digiti minimi (ADM) muscles are merged. Individual results are represented by the connected dots. Boxplots are included to compare results between groups.

periods preceding movement (Pogosyan et al., 2009). A third possibility is that TACS is only able to entrain corticospinal activity when falling in phase with endogenously generated beta activity, while entrainment may fade when stimulation presents random phases relative to cortical beta activity. Future studies may be able to test this possibility by driving TACS in a closed loop with estimates of ongoing cortical beta activity (Peles et al., 2020). Finally, the lack of entrainment observed at the level of MNs could also be caused by compensatory mechanisms at the spinal cord level countering TACS-driven corticospinal entrainment. This would imply the existence of neural projections to the MN pool able to compensate for the changes of descending corticospinal inputs and resist changes in the level of the IMC. There is evidence that just such a spinal circuit acts to reduce oscillations around 10 Hz which cause tremor (Koželj & Baker, 2014; Williams et al., 2010), but there is hitherto no evidence of anything similar acting for beta frequencies.

To simulate how changes in corticospinal beta entrainment affect MN activity, we used a simplified model of a MN pool receiving common inputs from a relatively small pool of corticospinal cells representing the fastest brain–muscle pathways (Firmin et al., 2014; Fritz et al., 1985; Lemon, 2008). This is motivated by previous works showing that brain oscillations projected to muscles travel through the fastest pathways (Ibáñez et al., 2021). Interestingly, when the model is run using experimentally observed levels of corticospinal entrainment to cortical beta rhythms in primates (Baker et al., 2003), the levels of intramuscular beta coherence resemble those found in human experiments (Castronovo et al., 2015; Negro et al., 2016). This supports the suitability of the model and allows us to use a realistic reference value to study the effects of corticospinal beta entrainment. Based on this, the model leads to two predictions about the effects of changes in corticospinal beta entrainment on MN activity. First, it shows that there is a nearly linear relationship between small deviations from the used beta reference level in the corticospinal inputs and the observed changes in the IMC function. Second, it shows that relatively small pools of MNs (10–30 MNs) can readily provide an optimal description of changes in the beta common inputs. This is a relevant outcome to validate the results obtained in real experiments and based on information from limited pools of motor units due to the limitations in extracting information from non-invasive recordings of muscle activity (Farina & Holobar, 2016; Holobar et al., 2014).

Several limitations should be considered in the present study. First, we did not use subject-specific current flow modelling and, therefore, induced currents may not have been equally effective across subjects (Evans et al., 2020). Since the stimulus intensities were similar to those in previous works finding positive results of stimulation (Guerra et al., 2016; Pogosyan et al., 2009; Vossen et al., 2015), we estimate that our group results faithfully represent the effects of TACS on MNs. Second, it is also not possible to determine the relevance of non-cortical common inputs to a MN pool, which may affect the strength with which cortical inputs are seen in pools of motor units. Since our simulations using beta modulation levels based on primate data led to beta IMC levels similar to those found in real experiments, we do not expect that there are other relevant non-cortical beta sources to the muscles. Third, TACS was delivered at fixed frequencies, while typically beta corticomuscular coherence can vary across subjects and covers a relatively wide range in the 20−30 Hz band (Witham et al., 2011). Future studies should assess how changes in the frequency of stimulation may lead to different outcomes (Huang et al., 2021). Since we did not find clear evidence for entrainment on a subject-by-subject level, we do not expect that this factor has a major impact on our conclusions. Finally, our results showing a lack of evidence of corticospinal entrainment are based on recordings during muscle contractions (otherwise we would not be able to process motor unit activity). Under these conditions, both cortical beta power and corticomuscular coherence are physiologically elevated, and this may have prevented these measures to be further enhanced by TACS given at beta. Given the large fluctuations that beta activity presents in the corticospinal system during sustained contractions (Echeverria-Altuna et al., 2021; Torrecillos et al., 2014), we consider that this factor should not have a major effect on our results.

Conclusion

We have proposed a method based on the non-invasive characterization of the firing activity of motor unit pools in a muscle to study TACS-driven neural entrainment of motor cortical outputs to the spinal cord and muscles. This was supported by realistic simulations suggesting that common inputs to MNs should be sensitive to changes in corticospinal entrainment. However, our experimental results indicate that TACS could not alter MN activity, which suggests that TACS-driven motor cortical entrainment may not be easy to achieve.

References

Asamoah, B., Khatoun, A., & Mc Laughlin, M. (2019). tACS motor system effects can be caused by transcutaneous stimulation of peripheral nerves. *Nature Communication*, **10**(1), 266.

Baker, S. N., & Lemon, R. N. (1998). Computer simulation of post-spike facilitation in spike-triggered averages of rectified EMG. *Journal of Neurophysiology*, **80**(3), 1391–1406.

Baker, S. N., Olivier, E., & Lemon, R. N. (1997). Coherent oscillations in monkey motor cortex and hand muscle EMG show task-dependent modulation. *Journal of Physiology*, **501**(1), 225–241.

Baker, S. N., Pinches, E. M., & Lemon, R. N. (2003). Synchronization in monkey motor cortex during a precision grip task. II. Effect of oscillatory activity on corticospinal output. *Journal of Neurophysiology*, **89**(4), 1941–1953.

Baker, S. N., Spinks, R., Jackson, A., & Lemon, R. N. (2001). Synchronization in monkey motor cortex during a precision grip task. I. Task-dependent modulation in single-unit synchrony. *Journal of Neurophysiology*, **85**(2), 869–885.

Bates, D., Mächler, M., Bolker, B. M., & Walker, S. C. (2015). Fitting linear mixed-effects models using lme4. *Journal of Statistical Software*, **67**, 148.

Beliaeva, V., Savvateev, I., Zerbi, V., & Polania, R. (2021). Toward integrative approaches to study the causal role of neural oscillations via transcranial electrical stimulation. *Nature Communication*, **12**(1), 1–12.

Booth, V., Rinzel, J., & Kiehn, O. (1997). Compartmental model of vertebrate motoneurons for Ca^{2+}-dependent spiking and plateau potentials under pharmacological treatment. *Journal of Neurophysiology*, **78**(6), 3371–3385.

Bräcklein, M., Barsakcioglu, D. Y., Del Vecchio, A., Ibáñez, J., & Farina, D. (2022). Reading and modulating cortical beta bursts from motor unit spiking activity. *Journal of Neuroscience*, **42**(17), 3611–3621.

Bräcklein, M., Ibáñez, J., Barsakcioglu, D., & Farina, D. (2021). Towards human motor augmentation by voluntary decoupling beta activity in the neural drive to muscle and force production. *Journal of Neural Engineering*, **18**(1), 016001.

Castronovo, A. M., Negro, F., Conforto, S., & Farina, D. (2015). The proportion of common synaptic input to motor neurons increases with an increase in net excitatory input. *Journal of Applied Physiology*, **119**(11), 1337–1346.

Dideriksen, J. L., Negro, F., Enoka, R., & Farina, D. (2012). Motor unit recruitment strategies and muscle properties determine the influence of synaptic noise on force steadiness. *Journal of Neurophysiology*, **107**(12), 3357–3369.

Echeverria-Altuna, I., Quinn, A. J., Zokaei, N., Woolrich, M. W., Nobre, A. C., & Van Ede, F. (2021). Transient beta activity and connectivity during sustained motor behaviour. *bioRxiv*.; https://doi.org/10.1101/2021.03.02.433514. bioRxiv

Enoka, R. (2008). Neuromechanics of human movement*ed*. Human Kinetics.

Evans, C., Bachmann, C., Lee, J. S. A., Gregoriou, E., Ward, N., & Bestmann, S. (2020). Dose-controlled tDCS reduces electric field intensity variability at a cortical target site. *Brain Stimulation*, **13**(1), 125–136.

Farina, D., & Holobar, A. (2016). Characterization of human motor units from surface EMG decomposition. *Proceedings of the IEEE*, **104**(2), 353–373.

Farina, D., & Negro, F. (2015). Common synaptic input to motor neurons, motor unit synchronization, and force control. *Exercise and Sport Sciences Reviews*, **43**(1), 23–33.

Farina, D., Negro, F., & Dideriksen, J. L. (2014). The effective neural drive to muscles is the common synaptic input to motor neurons. *Journal of Physiology*, **592**(16), 3427–3441.

Firmin, L., Field, P., Maier, M. A., Kraskov, A., Kirkwood, P. A., Nakajima, K., Lemon, R. N., & Glickstein, M. (2014). Axon diameters and conduction velocities in the macaque pyramidal tract. *Journal of Neurophysiology*, **112**(6), 1229–1240.

Fritz, N., Illert, M., Kolb, F. P., Lemon, R. N., Muir, R. B., Vanderburg, J., & Yamaguchi, T. (1985). The cortico-motoneuronal input to hand and forearm motoneurones in the anesthetized monkey. *Journal of Physiology*, **366**, 20.

Fu, L., Rocchi, L., Hannah, R., Xu, G., Rothwell, J. C., & Ibáñez, J. (2021). Corticospinal excitability modulation by pairing peripheral nerve stimulation with cortical states of movement initiation. *Journal of Physiology*, **599**(9), 2471–2482.

Gallego, J. A., Dideriksen, J. L., Holobar, A., Ibáñez, J., Pons, J. L., Louis, E. D., Rocon, E., & Farina, D. (2015). Influence of common synaptic input to motor neurons on the neural drive to muscle in essential tremor. *Journal of Neurophysiology*, **113**(1), 182–191.

Guerra, A., Pogosyan, A., Nowak, M., Tan, H., Ferreri, F., Di Lazzaro, V., & Brown, P. (2016). Phase dependency of the human primary motor cortex and cholinergic inhibition cancelation during beta tACS. *Cerebral Cortex*, **26**(10), 3977–3990.

Halliday, D. M. (2015). Nonparametric directionality measures for time series and point process data. *Journal of Integrative Neuroscience*, **14**(02), 253–277.

Helfrich, R. F., Schneider, T. R., Rach, S., Trautmann-Lengsfeld, S. A., Engel, A. K., & Herrmann, C. S. (2014). Entrainment of brain oscillations by transcranial alternating current stimulation. *Current Biology*, **24**(3), 333–339.

Holobar, A., Minetto, M. A., & Farina, D. (2014). Accurate identification of motor unit discharge patterns from high-density surface EMG and validation with a novel signal-based performance metric. *Journal of Neural Engineering*, **11**(1), 016008.

Huang, W. A., Stitt, I. M., Negahbani, E., Passey, D. J., Ahn, S., Davey, M., Dannhauer, M., Doan, T. T., Hoover, A. C., Peterchev, A. V., Radtke-Schuller, S., & Fröhlich, F. (2021). Transcranial alternating current stimulation entrains alpha oscillations by preferential phase synchronization of fast-spiking cortical neurons to stimulation waveform. *Nature Communication*, **12**(1), 3151. https://doi.org/10.1038/s41467-021-23021-2.

Hug, F., Avrillon, S., Del Vecchio, A., Casolo, A., Ibanez, J., Nuccio, S., Rossato, J., Holobar, A., & Farina, D. (2021). Analysis of motor unit spike trains estimated from high-density surface electromyography is highly reliable across operators. *Journal of Electromyography and Kinesiology*, **58**, 102548.

Ibáñez, J., Del Vecchio, A., Rothwell, J. C., Baker, S. N., & Farina, D. (2021). Only the Fastest Corticospinal Fibers Contribute to β Corticomuscular Coherence. *Journal of Neuroscience*, **41**(22), 4867–4879.

Jackson, A., Spinks, R. L., Freeman, T. C. B., Wolpert, D. M., & Lemon, R. N. (2002). Rhythm generation in monkey motor cortex explored using pyramidal tract stimulation. *Journal of Physiology*, **541**(3), 685–699.

Johnson, L., Alekseichuk, I., Krieg, J., Doyle, A., Yu, Y., Vitek, J., Johnson, M., & Opitz, A. (2020). Dose-dependent effects of transcranial alternating current stimulation on spike timing in awake nonhuman primates. *Science Advances*, **6**(36), 1–9.

Kar, K., & Krekelberg, B. (2012). Transcranial electrical stimulation over visual cortex evokes phosphenes with a retinal origin. *Journal of Neurophysiology*, **108**(8), 2173–2178.

Kasten, F. H., & Herrmann, C. S. (2019). Recovering brain dynamics during concurrent tACS-M/EEG: An overview of analysis approaches and their methodological and interpretational pitfalls. *Brain Topography*, **32**(6), 1013–1019.

Khatoun, A., Asamoah, B., & Mc Laughlin, M. (2017). Simultaneously excitatory and inhibitory effects of transcranial alternating current stimulation revealed using selective pulse-train stimulation in the rat motor cortex. *Journal of Neuroscience*, **37**(39), 9389–9402.

Koželj, S., & Baker, S. N. (2014). Different phase delays of peripheral input to primate motor cortex and spinal cord promote cancellation at physiological tremor frequencies. *Journal of Neurophysiology*, **111**(10), 2001–2016.

Kozyrev, V., Staadt, R., Eysel, U. T., & Jancke, D. (2018). TMS-induced neuronal plasticity enables targeted remodeling of visual cortical maps. *Pnas*, **115**(25), 6476–6481.

Kraskov, A., Baker, S. N., Soteropoulos, D. S., Kirkwood, P., & Lemon, R. N. (2019). The corticospinal discrepancy: Where are all the slow pyramidal tract neurons? *Cerebral Cortex*, **29**(9), 3977–3981.

Lafon, B., Henin, S., Huang, Y., Friedman, D., Melloni, L., Thesen, T., Doyle, W., Buzsáki, G., Devinsky, O., Parra, L. C., & Liu, A. A. (2017). Low frequency transcranial electrical stimulation does not entrain sleep rhythms measured by human intracranial recordings. *Nature Communication*, **8**(1), 1–14.

Lemon, R. N. (2008). Descending pathways in motor control. *Annual Review of Neuroscience*, **31**(1), 195–218.

MacGregor, R. J. (1987). *Neural and bain modeling*, 1st edn. Academic Press. Available at: https://linkinghub.elsevier.com/retrieve/pii/B9780124642607%D7;50019.

Negro, F., & Farina, D. (2011a). Linear transmission of cortical oscillations to the neural drive to muscles is mediated by common projections to populations of motoneurons in humans. *Journal of Physiology*, **589**(3), 629–637.

Negro, F., & Farina, D. (2011b). Decorrelation of cortical inputs and motoneuron output. *Journal of Neurophysiology*, **106**(5), 2688–2697.

Negro, F., Yavuz, U., & Farina, D. (2016). The human motor neuron pools receive a dominant slow-varying common synaptic input. *Journal of Physiology*, **594**(19), 5491–5505.

Neuling, T., Ruhnau, P., Weisz, N., Herrmann, C. S., & Demarchi, G. (2017). Faith and oscillations recovered: On analyzing EEG/MEG signals during tACS. *Neuroimage*, **147**, 960–963.

Noury, N., Hipp, J. F., & Siegel, M. (2016). Physiological processes non-linearly affect electrophysiological recordings during transcranial electric stimulation. *Neuroimage*, **140**, 99–109.

Noury, N., & Siegel, M. (2018). Analyzing EEG and MEG signals recorded during tES, a reply. *Neuroimage*, **167**, 53–61.

Nowak, M., Hinson, E., van Ede, F., Pogosyan, A., Guerra, A., Quinn, A., Brown, P., & Stagg, C. J. (2017). Driving human motor cortical oscillations leads to behaviorally relevant changes in local GABA a inhibition: A tACS-TMS study. *Journal of Neuroscience*, **37**(17), 4481–4492.

Paulus, W., Peterchev, A., & Ridding, M. C. (2013). *Transcranial electric and magnetic stimulation: Technique and paradigms*, 1st edn. Elsevier B.V.

Peles, O., Werner-Reiss, U., Bergman, H., Israel, Z., & Vaadia, E. (2020). Phase-specific microstimulation differentially modulates beta oscillations and affects behavior. *Cell Reports*, **30**(8), 2555–2566.e3.

Pogosyan, A., Gaynor, L. D., Eusebio, A., & Brown, P. (2009). Boosting cortical activity at beta-band frequencies slows movement in humans. *Current Biology*, **19**(19), 1637–1641.

Porter, R., & Lemon, R. (1995). *Corticospinal function and voluntary movement*. Oxford University Press. Available at: https://oxford.universitypressscholarship.com/view/10.1093/acprof:oso/9780198523758.001.0001/acprof-9780198523758.

R Development Core Team (2019). *R: A language and environment for statistical computing*. R Foundation for Statistical Computing.

Rosner, B. (2015). *Fundamentals of biostatistics*, (8th ed.). Cengage Learning.

Rossini, P., Burke, D., Chen, R., Cohen, L. G., Daskalakis, Z., Di Iorio, R., Di Lazzaro, V., Ferreri, F., Fitzgerald, P. B., George, M. S., Hallett, M., Lefaucheur, J. P., Langguth, B., Matsumoto, H., Miniussi, C., Nitsche, M. A., Pascual-Leone, A., Paulus, W., Rossi, S., … Ziemann, U. (2015). Non-invasive electrical and magnetic stimulation of the brain, spinal cord, roots and peripheral nerves: basic principles and procedures for routine clinical and research application. An updated report from an I.F.C.N. Committee. *Clinical Neurophysiology*, **126**(6), 1071–1107.

Torrecillos, F., Albouy, P., Brochier, T., & Malfait, N. (2014). Does the processing of sensory and reward-prediction errors involve common neural resources? Evidence from a frontocentral negative potential modulated by movement execution errors. *Journal of Neuroscience*, **34**(14), 4845–4856.

Varela, F. J., Lachaux, J. P., Rodriguez, E., & Martinerie, J. (2001). The brainweb: Phase synchronization and large-scale integration. *Nature Reviews Neuroscience*, **2**(4), 229–239.

Del Vecchio, A., Holobar, A., Falla, D., Felici, F., Enoka, R., & Farina, D. (2020). Tutorial: Analysis of motor unit discharge characteristics from high-density surface EMG signals. *Journal of Electromyography and Kinesiology*, **53**, 102426.

Violante, I. R., Li, L. M., Carmichael, D. W., Lorenz, R., Leech, R., Hampshire, A., Rothwell, J. C., & Sharp, D. J. (2017). Externally induced frontoparietal synchronization modulates network dynamics and enhances working memory performance. *Elife*, **6**, 1–22.

Vöröslakos, M., Takeuchi, Y., Brinyiczki, K., Zombori, T., Oliva, A., Fernández-Ruiz, A., Kozák, G., Kincses, Z. T., Iványi, B., Buzsaki, G., & Berényi, A. (2018). Direct effects of transcranial electric stimulation on brain circuits in rats and humans. *Nature Communication*, **9**(1), 483. https://doi.org/10.1038/s41467-018-02928-3.

Vossen, A., Gross, J., & Thut, G. (2015). Alpha power increase after transcranial alternating current stimulation at alpha frequency (a-tACS) reflects plastic changes rather than entrainment. *Brain Stimul*, **8**(3), 499–508.
Williams, E. R., & Baker, S. N. (2009a). Renshaw cell recurrent inhibition improves physiological tremor by reducing corticomuscular coupling at 10 Hz. *Journal of Neuroscience*, **29**(20), 6616–6624.
Williams, E. R., & Baker, S. N. (2009b). Circuits generating corticomuscular coherence investigated using a biophysically based computational model. I. Descending systems. *Journal of Neurophysiology*, **101**(1), 31–41.
Williams, E. R., Soteropoulos, D. S., & Baker, S. N. (2010). Spinal interneuron circuits reduce approximately 10-Hz movement discontinuities by phase cancellation. *PNAS*, **107**(24), 11098–11103.
Wischnewski, M., Schutter, D., & Nitsche, M. A. (2019). Effects of beta-tACS on corticospinal excitability: A meta-analysis. *Brain Stimulation*, **12**(6), 1381–1389.
Witham, C., Riddle, C. N., Baker, M. R., & Baker, S. N. (2011). Contributions of descending and ascending pathways to corticomuscular coherence in humans. *Journal of Physiology*, **589**(15), 3789–3800.

Additional information

Data availability statement

Data from this study will be made available to qualified investigators upon reasonable request to the corresponding author.

Competing interests

None declared.

Author contributions

Experiments performed at UCL. All authors approved the final version of the manuscript. All authors agree to be accountable for all aspects of the work. All authors qualify for authorship, and all those who qualify for authorship are listed. J.I.: Conceptualization, Methodology, Software, Formal analysis, Investigation, Writing – original draft, Writing – review & editing, Visualization. B.Z.: Investigation, Methodology, Writing – review & editing. K.B.: Investigation, Methodology, Writing – original draft, Writing – review & editing. L.R.: Methodology, Writing – review & editing, Visualization. A.D.V.: Conceptualization, Investigation, Writing – review & editing. D.S.: Conceptualization, Writing – review & editing. C.A.V.: Methodology, Formal Analysis. J.R., D.F., S.N.B.: Conceptualization, Resources, Writing – review & editing, Funding acquisition.

Funding

This work was supported by the European Research Council Synergy Grant Natural BionicS (Contract #810346). J.I. received the support from 'la Caixa' Foundation (ID 100010434; fellowship code LCF/BQ/PI21/11830018).

Acknowledgements

We thank Paul Hammond for building the experimental platform used to record forces generated by the tibialis anterior muscle.

Keywords

electromyography, motor neurons, movement, neuromodulation, transcranial alternating current stimulation

Supporting information

Additional supporting information can be found online in the Supporting Information section at the end of the HTML view of the article. Supporting information files available:

Statistical Summary Document
Peer Review History